Journal of Advanced Research 35 (2022) 129–140

Contents lists available at ScienceDirect

Journal of Advanced Research

journal homepage: www.elsevier.com/locate/jare

The link between deacetylation and hepatotoxicity induced by exposure to hexavalent chromium

Qingyue Yang [a,b], Bing Han [a], Siyu Li [a], Xiaoqiao Wang [a], Pengfei Wu [a], Yan Liu [a], Jiayi Li [a], Biqi Han [a], Ning Deng [a], Zhigang Zhang [a,b,*]

[a] College of Veterinary Medicine, Northeast Agricultural University, 600 Changjiang Road, Harbin 150030, China
[b] Heilongjiang Key Laboratory for Laboratory Animals and Comparative Medicine, 600 Changjiang Road, Harbin 150030, China

HIGHLIGHTS

- Cr(VI) can induce inflammatory, oxidative stress, and apoptosis in rat liver.
- Cr(VI) induces inflammatory response in the liver by inhibiting deacetylation.
- Oxidative stress caused by Cr(VI) is related to the inhibition of deacetylation.
- Cr(VI) aggravates hepatocyte apoptosis by inhibiting deacetylation in rats.
- Cr(VI) induces liver injury via inhibition of the deacetylation of Sirt1.

GRAPHICAL ABSTRACT

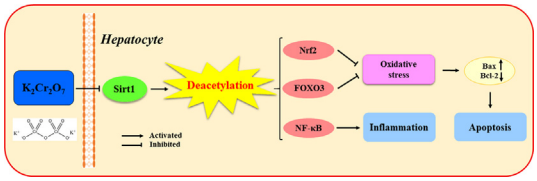

ARTICLE INFO

Article history:
Received 8 February 2021
Revised 31 March 2021
Accepted 4 April 2021
Available online 8 April 2021

Keywords:
Cr(VI)
Deacetylation
Sirt1
Oxidative stress
Apoptosis
Liver injury

ABSTRACT

Introduction: Hexavalent chromium (Cr(VI)), one of the toxic heavy metals, poses a serious threat to human and animal health. Protein acetylation regulates the structure and function of most proteins in a variety of ways. However, the hepatotoxicity of Cr(VI) and whether it is related to deacetylation remains largely unknown.

Objectives: We aimed to explore the link between the deacetylation of silent information regulator two ortholog 1 (Sirt1) and hepatotoxicity induced by Cr(VI) exposure, and to better clarify the biological mechanism of liver injury induced by Cr(VI).

Methods: We established a model of liver injury of $K_2Cr_2O_7$ by injecting rats intraperitoneally for 35 days continuously and adding resveratrol (Res) to further explore the link between deacetylation and hepatotoxicity.

Results: The results revealed that Cr(VI) induced inflammatory response and apoptosis in hepatocytes. Furthermore, Cr(VI) reduced Sirt1 expression and inhibited the deacetylation of Sirt1 to downstream key transcription factors, including nuclear factor erythroid 2-related factor 2 (Nrf2), Forkhead box O3 (FOXO3), and nuclear factor-kappa B (NF-κB). Conversely, when Res was administered as an activator of Sirt1, the deacetylation of Sirt1 was enhanced, and inflammatory response and apoptosis were significantly alleviated.

Peer review under responsibility of Cairo University.

* Corresponding author at: College of Veterinary Medicine, Northeast Agricultural University, No. 600 Changjiang Road, Harbin 150030, China.
E-mail address: zhangzhigang@neau.edu.cn (Z. Zhang).

https://doi.org/10.1016/j.jare.2021.04.002

Conclusion: In summary, this work firstly demonstrates that Cr(VI) induces liver injury in rat by inhibiting the deacetylation of Sirt1, which is of positive significance for protecting the natural environment and animal health from chronic Cr poisoning.

Introduction

Recently, hexavalent chromium (Cr(VI)) has aroused great interest among environmental health researchers due to Cr pollution in many countries around the world. Cr(VI), an environmental heavy metal pollutant, is widely present in industrial production processes such as metal smelting and leather processing, as well as automobile exhaust and cigarette smoke. The concentration of Cr(VI) in groundwater of California, Sao Paulo, Brazil, northern Italy, and Bangladesh ranging from 130 to 3000 μg/L [1–4], which is far higher than total Cr for the drinking water standard (50 μg/L) given by the World Health Organization [5]. German electroplating workers exposed to Cr for more than 30 years had a malignant tumor incidence of 97.1% and a lung cancer incidence of 95.4% [6]. After oral administration of 89 mg/kg of $K_2Cr_2O_7$ for 14 d, the rat mortality rate was 15% [7]. Occupational exposure to Cr(VI) affects the health of millions of workers worldwide, mainly through respiratory inhalation and skin contact [8]. Additionally, acute and chronic exposure to Cr(VI) shows neurotoxicity, genotoxicity, immunotoxicity, and carcinogenicity [9].

The liver is the main metabolic organ of toxic substances, and meanwhile, it is also the place where most heterogeneous biological compounds undergo biological transformation [10]. The liver is the main target organ of the body after Cr(VI) exposure, and Cr(VI) exposure via oral drinking water has increased the incidence and mortality of liver cancer in Greek workers [11]. It is worth noting that Cr(VI) can cause lipid peroxidation, DNA damage, and mitochondrial dysfunction in the liver [12]. Hence, the hepatotoxicity induced by Cr(VI) is of increasing concern, but the underlying developmental hepatotoxicity of Cr(VI) has not been fully investigated.

Apoptosis is an important toxicological phenomenon, which is a kind of spontaneous and orderly programmed cell death regulated by related genes [13]. Oxidative stress is a key factor for excessive cell apoptosis, and heavy metal toxicity often triggers a protective mechanism dominated by oxidative stress in cells in response to exogenous or oxidative damage [14]. Nuclear factor erythroid 2-related factor 2 (Nrf2) is essential to redox homeostasis and can activate a variety of cytoprotective genes, especially NAD(P)H quinone oxidoreductase-1 (NQO1) and heme oxygenase 1 (HO-1) [15]. Forkhead box O3 (FOXO3) is a forkhead transcription factor, which can regulate the transcription of target genes related to apoptosis, autophagy, cell cycle progression, and oxidative stress [16]. Also, inflammation also exacerbates the development of liver injury. Nuclear factor-kappa B (NF-κB), an inducible transcription factor with pleiotropic functions, is critically involved in the occurrence and development of inflammation which actively participates in the transcription of many pro-inflammatory factors, including interleukin 1β (IL-1β) and tumor necrosis factor-α (TNF-α) [17,18]. However, the exact relationship between Cr(VI)-induced liver injury and inflammation, as well as apoptosis has not yet been elucidated.

Acetylation is an important way of protein modification in eukaryotic cells, regulating the structure and function of most proteins in cells by affecting enzyme activity, stability, subcellular localization, and interaction with other molecules [19–21]. The post-translational acetylation of lysine residues ε-amino is an important form of acetylation, which can dynamically regulate post-transcriptional protein functions due to its reversibility [19]. Sirtuins are a family of NAD^+-dependent deacetylases known to remove acetyl groups from lysine residues in rapid response to environmental changes [22]. Among them, silent information regulator 1 (Sirt1) is the most characteristic member of the family, and it is believed to deacetylate some transcription factors such as FOXOs, NF-κB, and tumor suppressor p53, therefore participating in various pathophysiological processes including oxidative stress, gene silencing, DNA damage, and apoptosis [23]. Additionally, the deacetylation of Sirt1 is considered to be a key link in pivotal pathogenic mechanisms involving apoptosis and inflammation [24]. However, the link between the deacetylation of Sirt1 and hepatotoxicity induced by Cr(VI) remains unknown.

In our study, we investigated the hepatotoxicity induced by exposure to Cr(VI), and explored the link between the deacetylation of Sirt1 and Cr(VI)-induced liver injury in rats.

Materials and methods

Reagents and antibodies

Potassium dichromate ($K_2Cr_2O_7$) was the product of Tianjin Tianli Chemical Reagent Co., Ltd. (Tianjin, China). Carboxymethylcellulose (CMC) was obtained from Sinopharm Chemical Reagent Co., Ltd (Shanghai, China). Resveratrol (Res) was purchased from Xian Season Biotechnology Co., Ltd (Xian, China). Superoxide dismutase (SOD), malondialdehyde (MDA), and glutathione (GSH) detection kits were the products of Nanjing Jiancheng Bioengineering Co., Ltd. (China). Assay kits for Protein Extraction, Bicinchoninic acid (BCA), and Terminal deoxynucleotidyl transferase-mediated dUTP nick-end labeling (TUNEL) were supplied by Beyotime Biotechnology Research Institute (Jiangsu, China). Trizol reagent was the product of Invitrogen (Carlsbad, CA, USA). Antibodies to TNF-α, IL-1β, HO-1, NQO1, Bax, and Bcl-2 were acquired from Beijing Biosynthesis Biotechnology Co., Ltd. (China). Rabbit Polyclonal anti-acetylated-Lysine, anti- acetylated NF-κB p65 (Lys310), rabbit monoclonal anti-FOXO3, Sirt1, and superoxide dismutase 2 (SOD2) were the products of CST (Boston, MA, USA). Anti-acetylated Nrf2 (K599) was obtained from ImmunoWay Biotechnology (Newark, DE, USA). The antibody to GAPDH was got from Hangzhou Goodhere Biotechnology (China). ZSGB-BIO (Beijing, China) provided us with all the secondary antibodies.

Animals

All animal experiments were performed in accordance with the Ethical Committee for Animal Experiments of Northeast Agricultural University (Grant Number: 20190818). Thirty-five healthy male Wistar rats (weighing 170 ± 10 g, 6–8 w old) were from Harbin Veterinary Research Institute (Harbin, China). The rats were maintained under the standard laboratory conditions with controlled temperature (20–24 °C) and humidity (50%–60%), and were fed with food diet and water *ad libitum* in an alternating 12-h dark/12-h light cycle.

We established a rat liver injury model induced by $K_2Cr_2O_7$ and explore whether it is relevant to the deacetylation of Sirt1. The rats were randomly allocated to five groups (n = 7): control, $K_2Cr_2O_7$

low-dose, $K_2Cr_2O_7$ medium-dose, $K_2Cr_2O_7$ high-dose, and $K_2Cr_2O_7$ + Res groups. The rats of the control group were injected with normal saline intraperitoneally every day. The $K_2Cr_2O_7$ low-dose, medium-dose, and high-dose groups rats were intraperitoneally injected with 2, 4, and 6 mg/kg body weight/day of $K_2Cr_2O_7$, respectively. At the same time, rats in $K_2Cr_2O_7$ + Res group were administered $K_2Cr_2O_7$ at a dose of 4 mg/kg body weight/day by intraperitoneal injection and oral gavage with 100 mg/kg body weight/day Res (dissolved in CMC). The previous studies provided us with all the appropriate doses for rats [25,26]. After consecutive treatment for 35 d, the rats were starved for 24 h, anesthetized with ether and sacrificed. Fresh rat livers were then quickly frozen in liquid nitrogen, and then stored at −80 °C.

Histopathology

The sections of rat livers fixed in 4% paraformaldehyde were dehydrated with ethanol series, then the liver tissue samples were made into 3-μm paraffin sections and stained with hematoxylin and eosin (H&E). Finally, the liver tissue sections were examined by an Olympus light microscopy (Tokyo, Japan) for histopathological analysis.

Biochemical analysis

After collecting blood samples from the eyeballs, the serum was separated from fresh blood of rat by centrifugation at 3000 rpm for 10 min at 4 °C. The aspartate aminotransferase (AST) and alanine aminotransferase (ALT) of rat livers in each group were assessed with a Unicel DxC 800 Synchron chemistry system (Beckman, USA) [17].

Ultrastructural observation by transmission electron microscopy

As described previously [27], the liver sections (<1 mm^3) were fixed in 2.5% glutaraldehyde and phosphate 3 h at 4 °C, followed by staining with uranyl acetate and lead citrate. The ultrastructure images of liver tissue sections were obtained with a transmission electron microscope (TEM) (Hitachi H-7650, Tokyo, Japan).

Oxidative stress biomarker assay

To evaluate GSH and MDA content, and SOD activity, 10% liver tissue homogenates (2500 rpm 10 min, 4 °C), prepared in phosphate-buffered saline (pH 7.4), were used based on the instructions of corresponding commercial kits [28].

Comet assay

DNA damage was detected by lymphocytes isolated from rat blood. The samples were stained with 20 μg/mL of ethidium bromide after alkaline gel electrophoresis. Then, a fluorescence microscope (Olympus IX51; Nikon, Tokyo, Japan) was used to take pictures [29]. TriTek Comet Score Freeware v1.5 (TriTek Corp., Sumerduck, VA, USA) was used to analyze the images, and we used comet tail moments to score the severity of DNA damage in each group of blood lymphocytes.

TUNEL staining assay

Hepatocyte apoptosis was determined with a TUNEL kit as indicated by the manufacturer. Briefly, the samples were treated with 1% Triton X-100 and then blocked with 3% H_2O_2-carbinol for 15 min. Finally, the liver tissue samples were incubated with non-DNase protease K, followed by washing with PBS. Then the samples were combined with streptavidin-FITC and stained with DAPI at 25 °C for 5 min. A fluorescence microscopy (Nikon, Tokyo, Japan) was used to evaluate samples and record the proportion of apoptotic cells.

Western blot analysis

After the liver tissue was lysed in RIPA buffer containing the protease inhibitor phenylmethanesulfonyl fluoride on ice, the total protein in the liver tissue was extracted using the corresponding commercial kit, and the protein concentration was quantified by BCA method [30]. Briefly, the total protein was subjected to 12% gel SDS-PAGE and then transferred to polyvinylidene fluoride membranes. The blots were blocked in tris-buffered saline-Tween containing 5% skimmed milk powder for 2 h to bind non-specific sites, followed by overnight incubation at 4 °C with specific antibodies diluted to the appropriate concentration, and finally washed 6 times with TBST. Then these membranes were incubated with the appropriate secondary antibodies for 30 min at 37 °C. The protein expression levels were normalized to GAPDH. The intensity of protein bands was quantified by Image Pro-Plus 6.0 (Rockville, MD, USA).

Quantitative real-time PCR

The total RNA was isolated from liver tissue using Trizol reagent as described by a previous study [31]. A High Capacity cDNA Reverse Transcription kit (Vazyme, Nanjing, China) was used to reverse transcribe RNA into cDNA. According to the instructions of the SYBR Green RT-qPCR Supermix kit (Vazyme, Nanjing, China), the genes were combined with the corresponding specific primers (shown in Table 1) and the mRNA expression was quantitatively analyzed. PCR specificity was detected by both gel electrophoresis and the melting curve analysis. A Bio-Rad CFX96 touch (Hercules, CA, USA) was employed to analyze the relative mRNA levels normalized against β-actin mRNA levels. Calculations were performed by a comparative $2^{-\Delta\Delta CT}$ method.

Immunoprecipitation

The homogenates of rat liver tissues (100 μg) were diluted 4 times with immunoprecipitation buffer containing protease and phosphatase inhibitors and 0.5% NP-40, as previously described [32,33]. In brief, the obtained supernatant was co-incubated with 1–2 μg corresponding antibodies for 4 h, and then incubated with 25 μL protein A/G sepharose beads for 2 h at 4 °C with slow shaking. After the immunoprecipitation reaction, the samples of rat liver were centrifuged at 10,000 × *g*, and the obtained A/G beads were cleaned with 1 mL immunoprecipitation buffer 3–4 times. The immunoprecipitation proteins were released from the beads

Table 1
Primers sequences for qPCR.

Gene	Genebank Number	Primer sequences (5′→3′)
Sirt1	XM_039098755	F: AGT AAC AGT GAC AGT GGC ACA TGC R: CCT CCG TCA GCT CCA GAT CCT C
SOD2	NM_017051	F: CAC CGA GGA GAA GTA CCA R: ACA CAT CAA TCC CCA GCA
HO-1	XM_039097470	F: TAT CGT GCT CGC ATG AAC ACT CTG R: GTT GAG CAG GAA GGC GGT CTT AG
NQO1	NM_017000	F: AGA AGC GTC TGG AGA CTG TCT GG R: GAT CTG GTT GTC GGC TGG AAT GG

by boiling in SDS sample buffer at 100 °C for 5 min, and then used for western blot analysis.

Molecular modeling

SIRT1 three-dimensional structure (PDB ID: 5BTR) was obtained from the Protein Data Bank (http://www.rcsb.org). The three-dimensional structure of Res was downloaded from InDraw (Integle Information Technology Co., Ltd, Shanghai, China). The Sirt1 structure was molecularly docked with Res after removal of water molecules, hydrogenation, and residue correction. Sybyl-X 2.0 (Certara Inc., Princeton, NJ, USA) was used for molecular docking of the prepared Sirt1 protein with the small molecule ligand Res, taking into account the binding site of Res [34].

Protein-protein interaction analysis

In order to further understand the relationship between genes and identify more important genes, we conducted protein–protein interaction (PPI) network analysis. Specifically, we first uploaded the target genes to the STRING database (http://string-db.org/, Version 11.0), and then integrated the data retrieved from the string database with the identified genes to establish the target gene PPI network of the selected species.

Statistical analysis

SPSS 19.0 software (SPSS, Chicago, IL, USA) was applied for data statistics. Data were presented as mean ± SEM. Multiple groups were compared by performing one-way ANOVA following Tukey's post hoc test. *P* values <0.05 were considered to be statistically significant.

Results

$K_2Cr_2O_7$ induced liver damage

First, a classic rat model of $K_2Cr_2O_7$-induced liver injury was established to clarify the appropriate dose of $K_2Cr_2O_7$ and the effect of Sirt1 on liver injury. H&E histopathological observation showed that the liver structure in the control group was normal. However, in $K_2Cr_2O_7$ groups, the hepatocyte cords were arranged disorderly, and the sinusoids were dilated and hemorrhagic. Furthermore, hepatocyte swelling, nuclear shrinkage, as well as necrosis were also observed, and this effect was dose-dependent. Interestingly,

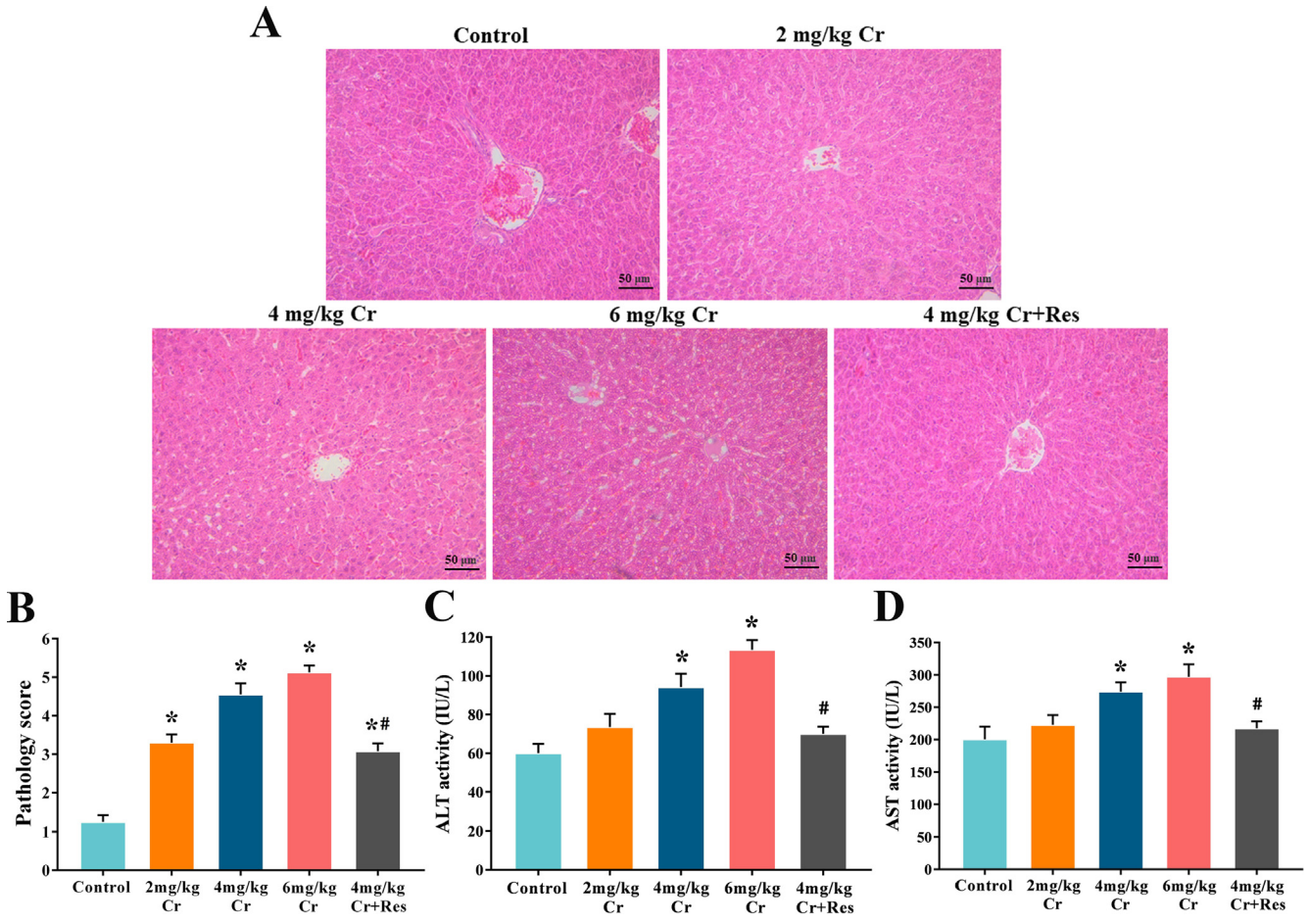

Fig. 1. Effect of exposure to $K_2Cr_2O_7$ on liver function in rat. (A) Paraffin sections of liver tissues from control, $K_2Cr_2O_7$ (2 mg/kg), $K_2Cr_2O_7$ (4 mg/kg), $K_2Cr_2O_7$ (6 mg/kg), and $K_2Cr_2O_7$ (4 mg/kg) + Res groups were stained with H&E staining (200 × magnification). (B) Pathology score of liver. (C) The activity of ALT. (D) The activity of AST. Values are mean ± SEM (n = 7). * Significantly different ($P < 0.05$) vs control group; # Significantly different ($P < 0.05$) vs $K_2Cr_2O_7$ (4 mg/kg) group.

the administration of Sirt1 activator completely restored the morphology of hepatocytes to normal levels and prevented liver damage (Fig. 1A, B).

Then, AST and ALT are important indicators to measure the degree of liver damage. Compared to the control group, the activities of AST and ALT increased in a dose-dependent manner, and this effect was significantly alleviated by Sirt1 activator treatment (Fig. 1C, D).

Finally, TEM was used to analyze the ultrastructure of liver tissues. The results clearly showed that the mitochondrial structure

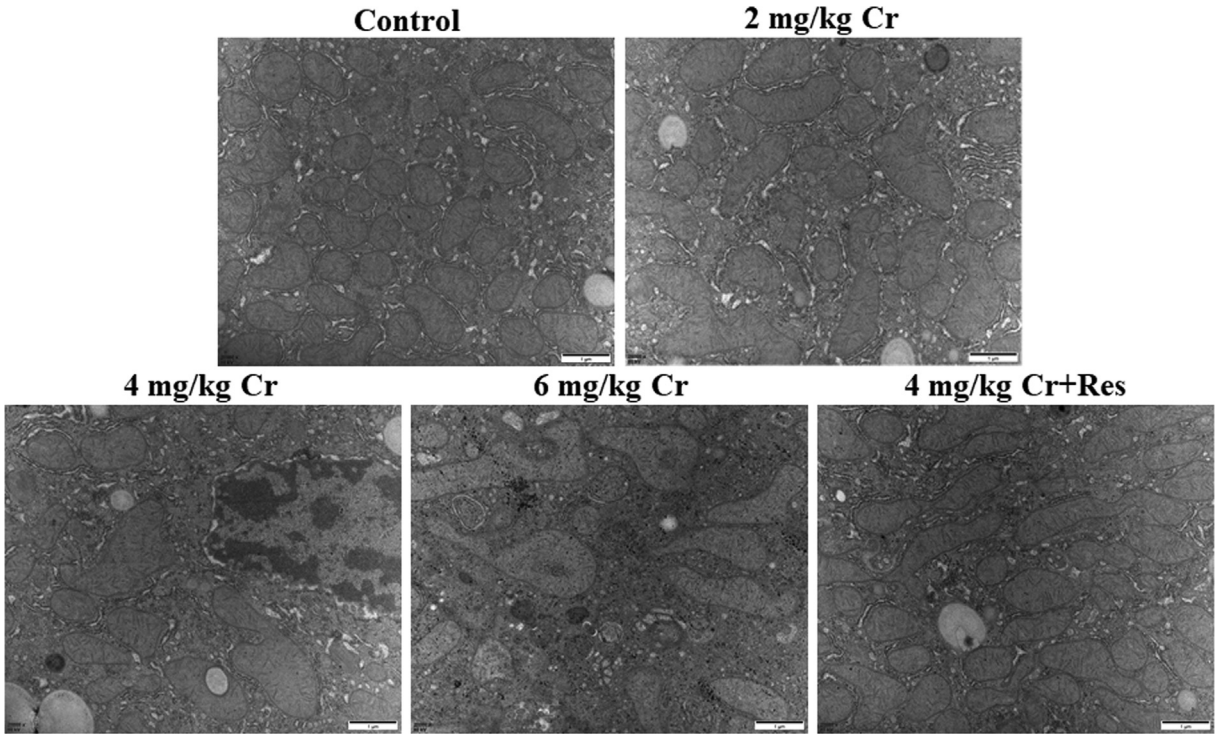

Fig. 2. Effect of exposure to $K_2Cr_2O_7$ on ultrastructure of rat liver. Ultrastructural changes of liver tissues from control, $K_2Cr_2O_7$ (2 mg/kg), $K_2Cr_2O_7$ (4 mg/kg), $K_2Cr_2O_7$ (6 mg/kg), and $K_2Cr_2O_7$ (4 mg/kg) + Res groups were observed by transmission electron microscopy. 20000 × magnification.

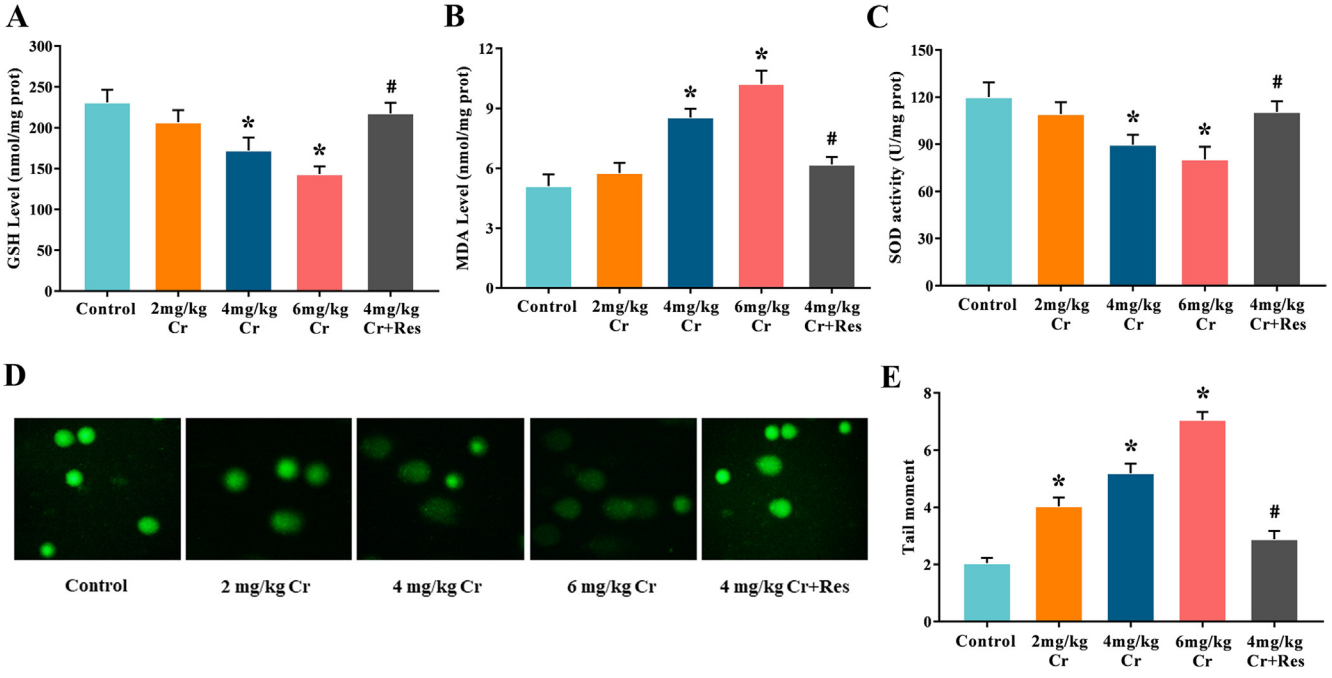

Fig. 3. Effect of exposure to $K_2Cr_2O_7$ on oxidative stress and DNA damage in rat liver. (A) The concentration of GSH. (B) The level of MDA. (C) The activity of SOD. (D) Representative comet assay images of leukocytes collected from 5 groups are shown; bars = 50 μm. (E) The quantification of tail moment. Data are the mean ± SEM (n = 7). * Significantly different ($P < 0.05$) vs control group; # Significantly different ($P < 0.05$) vs $K_2Cr_2O_7$ (4 mg/kg) group.

of the control liver was in consonance with the Res + $K_2Cr_2O_7$ co-treatment group. Specifically, the mitochondrial structure was clear, complete, and oval. In $K_2Cr_2O_7$ groups, mitochondrial swelling along with cristae fracture or even disappearance was noticed in hepatocytes in a dosage-dependent manner. Notably, the situation of $K_2Cr_2O_7$-induced liver injury was reversed by Sirt1 activator treatment (Fig. 2).

$K_2Cr_2O_7$ induced liver oxidative stress and DNA damage

In the model group, GSH content and SOD activity decreased while MDA level increased, and this effect was in a $K_2Cr_2O_7$ dose-dependent manner. Additionally, Sirt1 activator administration greatly alleviated the $K_2Cr_2O_7$-induced MDA content, restored SOD activity, and maintained GSH concentration in the liver (Fig. 3A-C).

Comet assay was performed to access the DNA damage in rats. Compared to the control group, the hemolymph cell tail distance in $K_2Cr_2O_7$ treatment groups significantly increased, and it was dose-related. However, this could be significantly resisted by the addition of Sirt1 activator (Fig. 3D, E).

$K_2Cr_2O_7$ induced hepatocyte apoptosis

Apoptosis of hepatocytes was detected by TUNEL staining. In the $K_2Cr_2O_7$ model groups, the proportion of hepatocyte apoptosis was gradually increased compared with the control group, while Sirt1 activator administration greatly reversed the increase of apoptosis-positive cells and decreased the apoptosis rate (Fig. 4A, B).

Western blot results showed that $K_2Cr_2O_7$-treatment dose-dependently increased Bax and decreased Bcl-2 expression levels contrasted to the control liver, while this effect was reversed by Sirt1 supplementation, which revealed that Cr(VI)-induced hepatocyte apoptosis could be alleviated after Sirt1 activator supplement (Fig. 4C, D, Fig. S1).

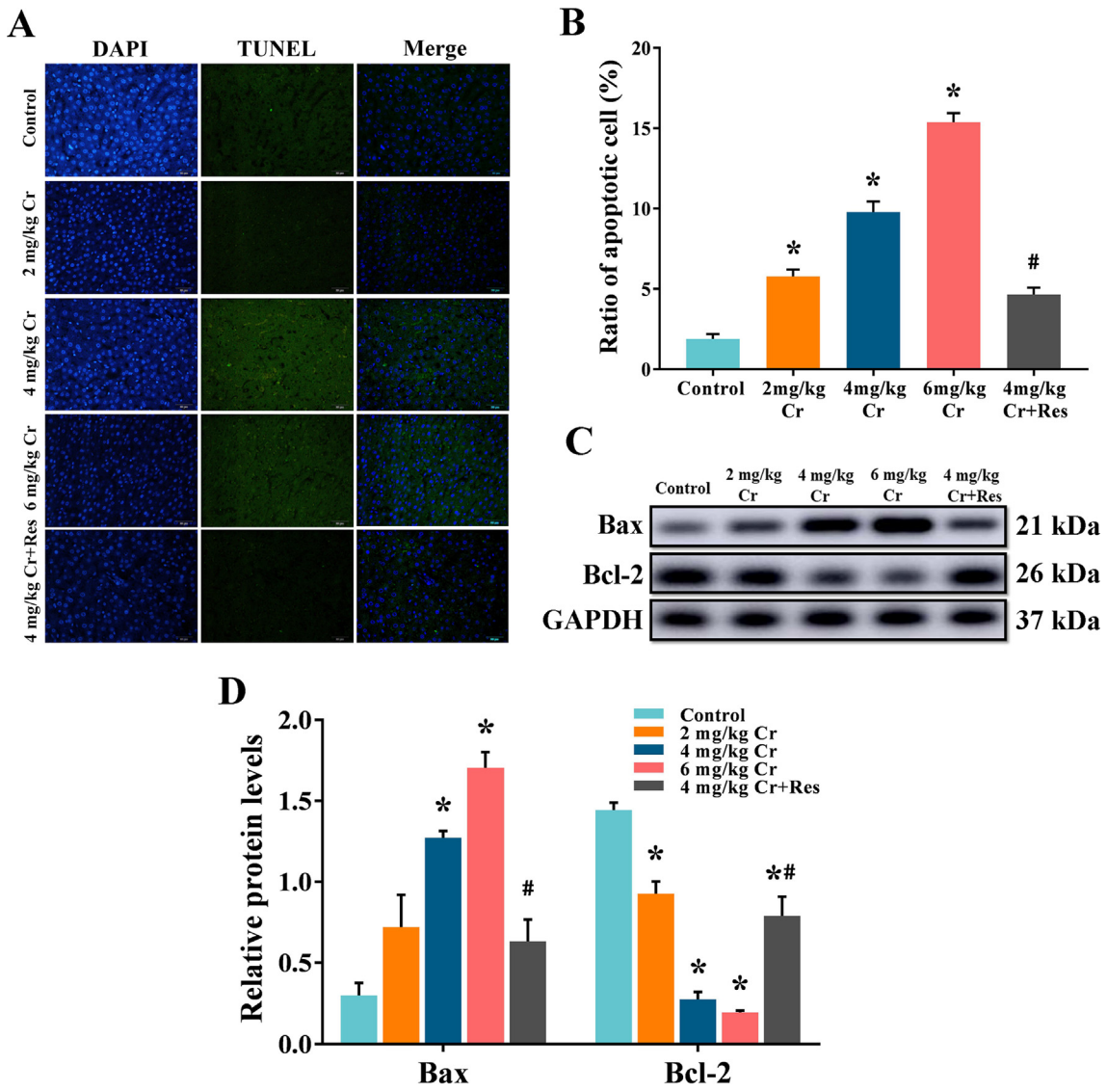

Fig. 4. Effect of exposure to $K_2Cr_2O_7$ on hepatocyte apoptosis in rat. Representative TUNEL images (400 × magnification). (B) Quantitation of TUNEL analysis. Data are the mean ± SEM. (C) The relative protein levels of Bax and Bcl-2 in the liver, and (D) values of quantitative analysis. Values are mean ± SEM (n = 4). * Significantly different ($P < 0.05$) vs control group; # Significantly different ($P < 0.05$) vs $K_2Cr_2O_7$ (4 mg/kg) group.

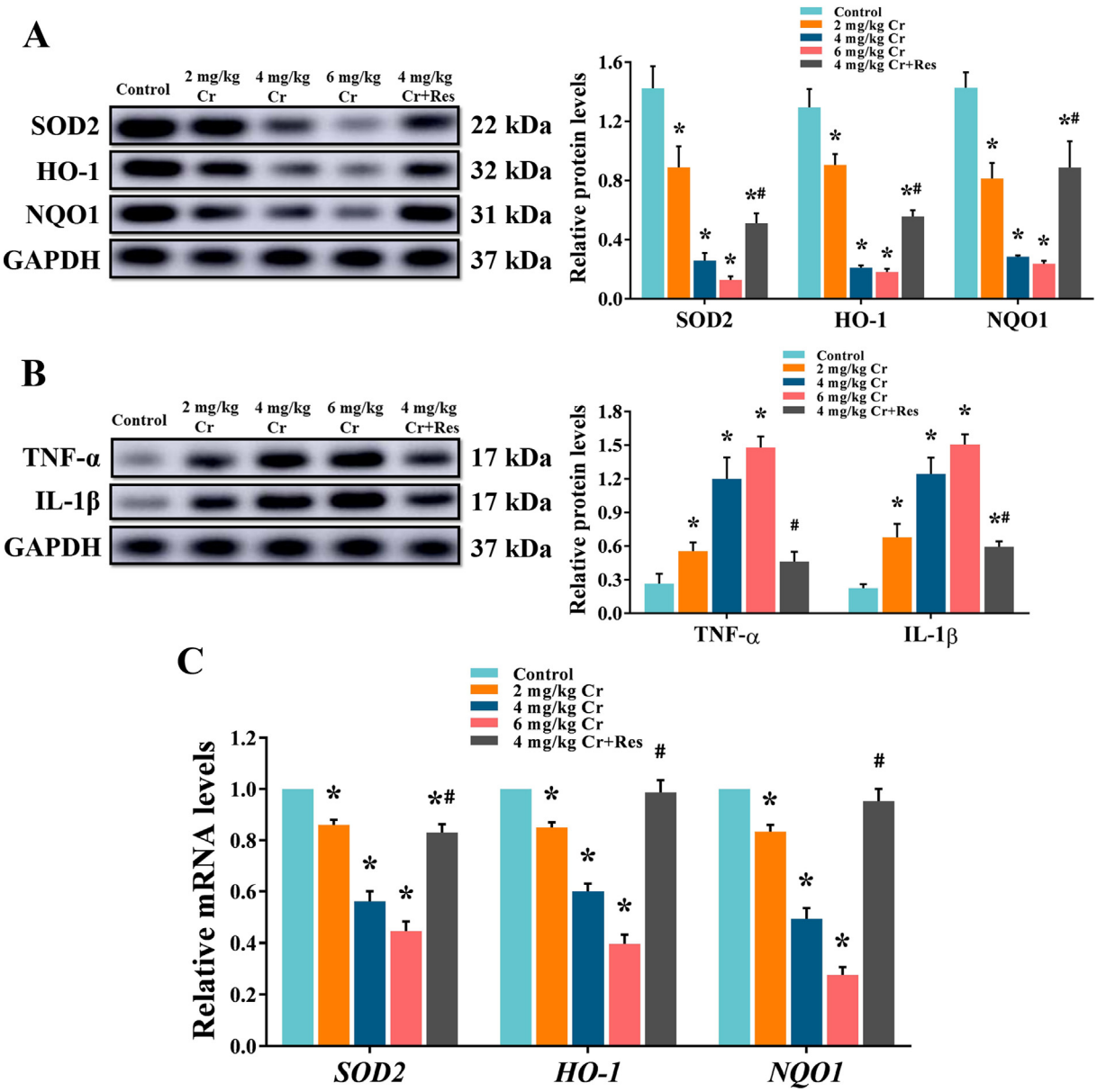

Fig. 5. Effect of exposure to $K_2Cr_2O_7$ on oxidative stress and inflammatory response in rat liver. (A) The relative protein levels of SOD2, HO-1, and NQO1. Values are mean ± SEM (n = 4). (B) The relative protein levels of TNF-α and IL-1β. Values are mean ± SEM (n = 4). (C) The relative mRNA levels of SOD2, HO-1, and NQO1 in rat liver were detected by qRT-PCR. Values are mean ± SEM (n = 7). * Significantly different ($P < 0.05$) vs control group; # Significantly different ($P < 0.05$) vs $K_2Cr_2O_7$ (4 mg/kg) group.

$K_2Cr_2O_7$ reduced the expression levels of antioxidant enzymes in rat liver

Western blot and qRT-PCR were used for quantitative analysis of oxidative stress-related antioxidant enzymes, including HO-1, NQO1, and SOD2 in liver tissue extracts. The results revealed that compared with the control liver, $K_2Cr_2O_7$ dramatically inhibited the expression of antioxidant enzymes, and it was dose-related. However, this suppressive effect was significantly alleviated in Sirt1 activator-treated rats (Fig. 5A, C, Fig. S2).

$K_2Cr_2O_7$ promoted inflammatory response in rat liver

Quantification of TNF-α and IL-1β in the extract of liver tissues showed that $K_2Cr_2O_7$ exposure significantly increased protein production compared to liver tissue levels in the control group, and it was dose-related. While in the Res + $K_2Cr_2O_7$ co-treatment liver, Sirt1 activator supplement alleviated $K_2Cr_2O_7$-induced inflammation response (Fig. 5B).

$K_2Cr_2O_7$ decreased the expression of Sirt1 and reduced the deacetylation of FOXO3, Nrf2, and NF-κB in rat liver

To examine the role of Sirt1 deacetylation in the hepatotoxicity of Cr(VI), we quantified the production of Sirt1 and the acetylation level of its downstream transcription factors by immunoprecipitation and western blot. We found that $K_2Cr_2O_7$ exposure markedly inhibited the production of Sirt1 and increased the acetylation levels of FOXO3, Nrf2, as well as NF-κB. When Res was given as a clear activator of Sirt1, the production of Sirt1 was increased and the levels of ac-FOXO3, ac-Nrf2, and ac-NF-κB were decreased (Fig. 6, Fig. S3).

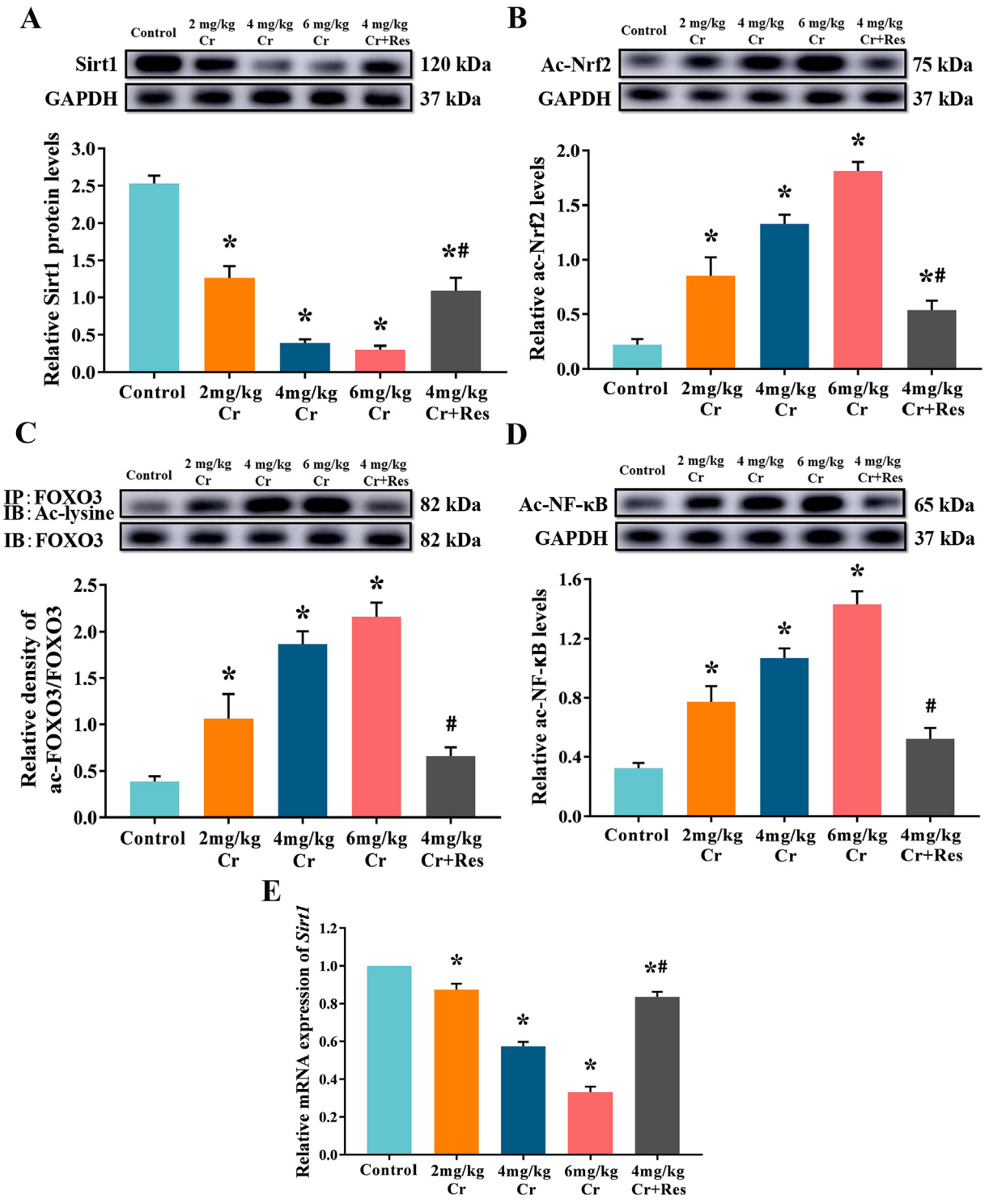

Fig. 6. Effect of exposure to $K_2Cr_2O_7$ on Sirt1 and its deacetylation in rat liver. (A) The relative protein levels of Sirt1. Values are mean ± SEM (n = 4). (B) The relative acetylated Nrf2 levels. Values are mean ± SEM (n = 4). (C) The relative acetylated FOXO3 levels. Immunoblotting for acetyl-lysine was performed on FOXO3 immunoprecipitates prepared at the indicated times. Values are mean ± SEM (n = 4). (D) The relative acetylated NF-κB levels. Values are mean ± SEM (n = 4). (E) The relative mRNA levels of Sirt1 in rat liver were detected by qRT-PCR. Values are mean ± SEM (n = 7). * Significantly different ($P < 0.05$) vs control group; # Significantly different ($P < 0.05$) vs $K_2Cr_2O_7$ (4 mg/kg) group. Ac-lysine: acetylated-Lysine; IP: immunoprecipitation; IB immunoblot analysis.

Docking modeling: Res interacts with Sirt1

Molecular docking showed that Res interacted with Sirt1 (Fig. 7A), and the relative binding site was shown in Fig. 7B. These results indicated that Res activates Sirt1 through direct interaction with Sirt1, enhancing the deacetylation of Sirt1.

PPI analysis

The PPI network of genes associated with oxidative stress, inflammation, and apoptosis was constructed to further verify our conjecture. The dynamic clusters were shown in Fig. 7C, including Sirt1, FOXO3, Nrf2, NF-κB, HO-1, NQO1, SOD2, TNF-α,

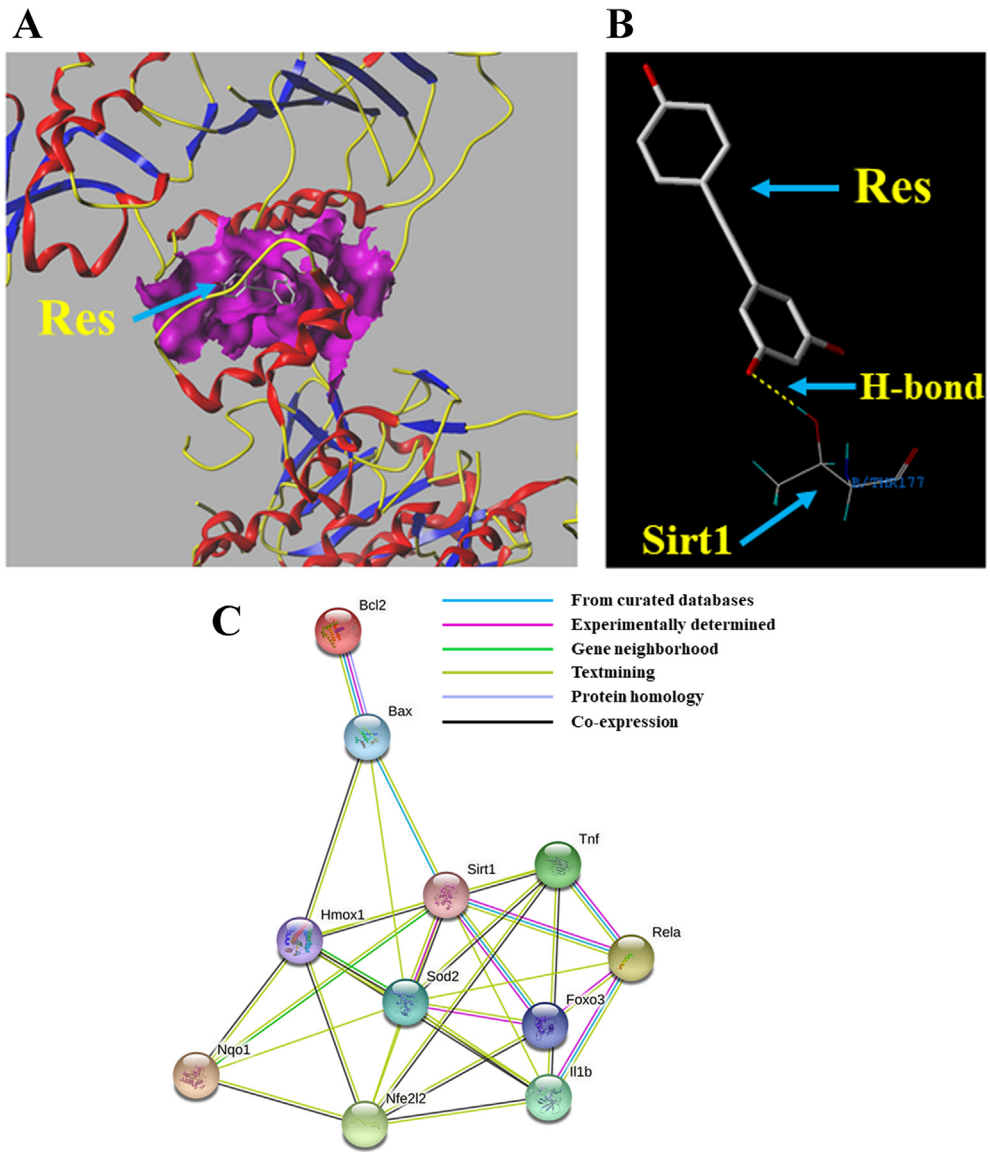

Fig. 7. Docking modeling for Res and Sirt1, and PPI analysis. (A) 3D molecular model of Res docking pose in the binding pocket of Sirt1. (B) 2D molecular docking model of the binding site of Res and Sirt1. The H-bonds are represented by yellow dotted lines. (C) Protein network of proteins regulated between Sirt1, oxidative stress-related genes, apoptosis-related genes, and inflammation-related genes expressed in rat liver. Nrf2 (Nfe212); Hmox1 (HO-1); Nqo1(NQO1); Tnf (TNF-α); IL1b (IL-1β); Rela (NF-κB).

IL-1β, Bax, and Bcl-2. The functional interaction network revealed the close relationship between Sirt1 and inflammation, as well as oxidative stress-mediated apoptosis.

Discussion

With the development of heavy and light industries, Cr pollution in the environment has become increasingly serious. Cr(VI) can cause serious harm in nature through various food chains and continuous bioaccumulation, as well as pose an indirect threat to animals and human health by affecting the water and air quality in the environment. Several studies have also implicated hepatocytes are more susceptible to Cr toxicity than other cells. Emerging data have revealed that protein deacetylation modification plays a key role in the pathogenesis of various toxicants such as heavy metals, acetaminophen, and particulate matter [35–37]. Therefore, it is of great meaning for us to explore the potential role of deacetylation in the toxicity of Cr in the mammalian liver. In our study, the results clearly showed that exposure to Cr(VI) leads to liver lesions and abnormal liver function. In addition, Cr(VI) also induces apoptosis and inflammatory response by inhibiting Sirt1 deacetylation. Our research firstly reveals the relationship between deacetylation and inflammatory response, as well as apoptosis induced by Cr(VI), laying a foundation for a better understanding of Cr toxicity.

It is worth noting that hepatocellular damage is not only due to the destruction of toxins but also due to the inflammatory response of hepatocytes under stress. Many protein functions are modulated by post-transcriptional modifications, such as acetylation, methylation, and phosphorylation, including NF-κB [38]. Furthermore, acetylated NF-κB exhibits stronger transcriptional activity and promotes the release of downstream pro-inflammatory cytokines [39]. Interestingly, Sirt1-mediated deacetylation prevents acetylated NF-κB-p65 from binding to the DNA promoter, leading to inactivation of NF-κB-p65, and reduces the transcriptional activity of NF-κB [40–42]. A previous report indicated that metal nanoparticles induced inflammation by regu-

lating Sirt1 through NF-κB-p65 deacetylation [43]. Therefore, we speculate that the Sirt1-mediated NF-κB deacetylation mechanism may also be involved in hepatotoxicity induced by Cr(VI) exposure. Importantly, in this study, we found that Cr(VI) exposure increased the level of acetylated NF-κB-p65 and up-regulated proinflammatory factor IL-1β and TNF-α by inhibiting the deacetylation of Sirt1 in the liver, consequently resulting in an inflammatory response. The deacetylation level of NF-κB-p65 increased and the activity of inflammatory factors decreased following Res treatment, and these effects were dependent on the presence of Sirt1 deacetylation, which provides new insights into the detoxification process of Cr(VI). Collectively, the deacetylation of Sirt1 may play a critical role in the inflammatory response induced by Cr(VI) exposure in rat liver.

Apoptosis is considered to be essential for maintaining tissue homeostasis and normal function and actively participates in the pathogenesis of a variety of heavy metals, such as lead, inorganic mercury, and Cr(VI) [26,29,44]. Oxidative stress not only causes DNA damage in cells but also participates in the regulation of apoptosis through the mitochondrial endogenous apoptosis pathway regulated by the pro-apoptotic protein (Bax) and the anti-apoptotic protein (Bcl-2) [26]. Combined with comet test and oxidative stress indicators, our findings illustrate that hepatocyte apoptosis induced by Cr(VI) may result from oxidative stress, which finally contributes to liver injury. The deacetylation of Sirt1 is closely related to oxidative stress and apoptosis. For instance, NiO induced p53 hyperacetylation and Bax overexpression via inhibiting the deacetylation of Sirt1 in BEAS-2B bronchial lung epithelial cells [45]. Moreover, Zhao et al. (2019) also found that Mn induced the increase of acetylated FOXO3 by down-regulating Sirt1 and activated the Bim/PUMA axis, leading to the apoptosis of PC12 cells in rats [46]. Together, the deacetylation of Sirt1 may be involved in oxidative stress-mediated apoptosis induced by Cr(VI) exposure.

Studies have strongly demonstrated that the Nrf2 system plays a pivotal role in a variety of toxic reactions induced by Cr(VI) [26,47]. The antioxidant function of the Nrf2 system is regulated by the acetylation-deacetylation state of Nrf2 [48]. As a key substrate of the deacetylase Sirt1, Nrf2 is deacetylated by Sirt1 to increase the expression of Nrf2 and downstream antioxidant genes, which enhances the stability of the Nrf2 system, thereby improving the antioxidant capacity [49,50]. Therefore, we put forward a reasonable conjecture that Nrf2, which is hyperacetylated by Sirt1, may be involved in hepatotoxicity induced by Cr(VI) exposure. Consistent with previous studies, our data confirm that Cr(VI) leads to high levels of ac-Nrf2 and lower levels of NQO1 and HO-1 by inhibiting Sirt1, which leads to excessive hepatocyte apoptosis by inducing the outbreak of oxidative stress in hepatocytes.

In addition to the Nrf2 system, FOXO3 also plays a beneficial role in anti-oxidative stress processes in a variety of cells [51,52]. Pieces of evidence have been accumulating that ac-FOXO3 is more likely to induce apoptosis, while deacetylated FOXO3 has higher transcriptional activity and stronger antioxidant capacity [53,54]. Of note, as the primary regulator of FOXO3, Sirt1 not only up-regulates FOXO3 expression through deacetylating and increases transcription of downstream antioxidant enzymes to resist oxidative stress but also prevents excessive cell death induced by FOXO3 [55]. Shang et al. (2016) found that zearalenone hyperacetylated FOXO3 by reducing Sirt1 expression, inducing oxidative stress, and increasing the expression rate of Bax/Bcl-2, which eventually caused excessive apoptosis of the human embryo kidney (HEK) 293 cell [56]. Based on these reports, our results suggest that Cr (VI) may also hyperacetylate FOXO3 by inhibiting Sirt1, leading to oxidative stress-mediated apoptosis.

Interestingly, after the administration of Sirt1 activator (Res), the acetylation was significantly inhibited and liver injury was reversed, suggesting that Res may have a potential therapeutic effect on Cr(VI)-induced liver injury. Thus, Cr(VI) exacerbates oxidative stress-mediated apoptosis by inhibiting the deacetylation of Nrf2 and FOXO3 by Sirt1 and hence plays a central role in the development of hepatotoxicity induced by Cr(VI) exposure.

Conclusion

All in all, our study firstly demonstrates the specific role of deacetylation in hepatotoxicity induced by Cr(VI) exposure. Specifically, Cr(VI) inhibited the deacetylation of Sirt1, which in turn triggers an inflammatory response and stress-mediated apoptosis, ultimately leading to liver injury in rat. These findings improve the understanding of hepatotoxicity induced by Cr(VI) and have important implications for public health and environmental safety.

CRediT authorship contribution statement

Qingyue Yang: Conceptualization, Methodology, Data curation, Writing - original draft. **Bing Han:** Conceptualization, Methodology, Investigation, Formal analysis. **Siyu Li:** Conceptualization, Methodology, Methodology, Data curation. **Xiaoqiao Wang:** Conceptualization, Methodology, Formal analysis. **Pengfei Wu:** Methodology, Validation. **Yan Liu:** Software, Formal analysis. **Jiayi Li:** Conceptualization, Investigation. **Biqi Han:** Methodology. **Ning Deng:** Software. **Zhigang Zhang:** Conceptualization, Methodology, Project administration, Writing - review & editing, Funding acquisition.

Declaration of Competing Interest

The authors declare that they have no known competing financial interests or personal relationships that could have appeared to influence the work reported in this paper.

Acknowledgement

This work was funded by the National Natural Science Foundation of China (31972754).

Compliance with Ethics Requirements

All Institutional and National Guidelines for the care and use of animals (fisheries) were followed.

All animal experiments were performed in accordance with the Ethical Committee for Animal Experiments of Northeast Agricultural University. The ethical committee number for the study is 20190818.

Appendix A. Supplementary material

Supplementary data to this article can be found online at https://doi.org/10.1016/j.jare.2021.04.002.

References

[1] Pellerin C, Booker SM. Reflections on hexavalent chromium: health hazards of an industrial heavyweight. Environ Health Perspect 2000;108:A402–7. doi: https://doi.org/10.1289/ehp.108-a402.

[2] Bertolo R, Bourotte C, Hirata R, Marcolan L, Sracek O. Geochemistry of natural chromium occurrence in a sandstone aquifer in Bauru Basin, Sao Paulo State, Brazil. Appl Geochem 2011;26:1353–63. doi: https://doi.org/10.1016/j.apgeochem.2011.05.009.

[3] Slejko FF, Petrini R, Lutman A, Forte C, Ghezzi L. Chromium isotopes tracking the resurgence of hexavalent chromium contamination in a past-contaminated area in the Friuli Venezia Giulia Region, northern Italy. Isot, Environ Health Stud 2019;55:56–69. doi: https://doi.org/10.1080/10256016.2018.1560278.
[4] Khan A, Michelsen N, Marandi A, Hossain R, Hossain MA, Roehl KE, et al. Processes controlling the extent of groundwater pollution with chromium from tanneries in the Hazaribagh area, Dhaka, Bangladesh. Sci Total Environ 2020;710:. doi: https://doi.org/10.1016/j.scitotenv.2019.136213136213.
[5] World Health Organization. Guidelines for Drinking-Water Quality, Fourth Edition Incorporating the First Addendum (WWW Document). 2017. https://www.who.int/publications/i/item/9789241549950
[6] Becker N, Claude J, Frentzel-Beyme R. Cancer risk of arc welders exposed to fumes containing chromium and nickel. Scand J Work Environ Health 1985;11:75–82. doi: https://doi.org/10.5271/sjweh.2242.
[7] Wilbur S, Abadin H, Fay M, Yu D, Tencza B, Ingerman L, et al. Toxicological Profile for Chromium. Agency for Toxic Substances and Disease Registry (US). Atlanta (GA) 2012.
[8] Zhao MD, Xu J, Li A, Mei YY, Ge XY, Liu XL, et al. Multiple exposure pathways and urinary chromium in residents exposed to chromium. Environ Int 2020;141:. doi: https://doi.org/10.1016/j.envint.2020.105753105753.
[9] Wang ZS, Yang CF. Metal carcinogen exposure induces cancer stem cell-like property through epigenetic reprograming: A novel mechanism of metal carcinogenesis. Semin Cancer Biol 2019;57:95–104. doi: https://doi.org/10.1016/j.semcancer.2019.01.002.
[10] Elshazly MO, Morgan AM, Ali ME, Abdel-Mawla E, Abd El-Rahman SS. The mitigative effect of *Raphanus sativus* oil on chromium-induced geno- and hepatotoxicity in male rats. J Adv Res 2016;7:413–21. doi: https://doi.org/10.1016/j.jare.2016.02.008.
[11] Linos A, Petralias A, Christophi CA, Christoforidou E, Kouroutou P, Stoltidis M, et al. Oral ingestion of hexavalent chromium through drinking water and cancer mortality in an industrial area of Greece-an ecological study. Environ Health 2011;10:50. doi: https://doi.org/10.1186/1476-069X-10-50.
[12] Yang QY, Han B, Xue JD, Lv YY, Li SY, Liu Y, et al. Hexavalent chromium induces mitochondrial dynamics disorder in rat liver by inhibiting AMPK/PGC-1α signaling pathway. Environ Pollut 2020;265:. doi: https://doi.org/10.1016/j.envpol.2020.114855114855.
[13] Liu BY, Yu HX, Baiyun RQ, Lu JJ, Li SY, Bing QZ, et al. Protective effects of dietary luteolin against mercuric chloride-induced lung injury in mice: Involvement of AKT/Nrf2 and NF-κB pathways. Food Chem Toxicol 2018;113:296–302. doi: https://doi.org/10.1016/j.fct.2018.02.003.
[14] Guo QW, Liu YX, Jia Q, Zhang G, Fan HM, Liu LD, et al. Ultrahigh sensitivity multifunctional nanoprobe for the detection of hydroxyl radical and evaluation of heavy metal induced oxidative stress in live hepatocyte. Anal Chem 2017;89:4986–93. doi: https://doi.org/10.1021/acs.analchem.7b00306.
[15] Li SY, Zheng XY, Zhang XY, Yu HX, Han B, Lv YY, et al. Exploring the liver fibrosis induced by deltamethrin exposure in quails and elucidating the protective mechanism of resveratrol. Ecotoxicol Environ Saf 2021;207:. doi: https://doi.org/10.1016/j.ecoenv.2020.111501111501.
[16] Liu Y, Ao X, Ding W, Ponnusamy M, Wu W, Hao XD, et al. Critical role of FOXO3a in carcinogenesis. Mol Cancer 2018;17:104. doi: https://doi.org/10.1016/j.semcancer.2019.01.002.
[17] Lv YY, Bing QZ, Lv ZJ, Xue JD, Li SY, Han B, et al. Imidacloprid-induced liver fibrosis in quails via activation of the TGF-β1/Smad pathway. Sci Total Environ 2020;705:. doi: https://doi.org/10.1016/j.scitotenv.2019.135915135915.
[18] Hamed MAA, Ahmed SAA, Khaled HM. Efficiency of diagnostic biomarkers among colonic schistosomiasis Egyptian patients. Mem Inst Oswaldo Cruz 2011;106:322–9. doi: https://doi.org/10.1590/s0074-02762011000300011.
[19] Cameron AM, Lawless SJ, Pearce EJ. Metabolism and acetylation in innate immune cell function and fate. Semin Immunol 2016;28:408–16. doi: https://doi.org/10.1016/j.smim.2016.10.003.
[20] Dai J, Huang YJ, He XH, Zhao M, Wang XZ, Liu ZS, et al. Acetylation blocks cGAS activity and inhibits self-DNA-induced autoimmunity. Cell 2019;176:1447–60. doi: https://doi.org/10.1016/j.cell.2019.01.016.
[21] Narita T, Weinert BT, Choudhary C. Functions and mechanisms of non-histone protein acetylation. Nat Rev Mol Cell Biol 2019;20:156–74. doi: https://doi.org/10.1038/s41580-018-0081-3.
[22] Houtkooper RH, Pirinen E, Auwerx J. Sirtuins as regulators of metabolism and healthspan. Nat Rev Mol Cell Biol 2012;13:225–38. doi: https://doi.org/10.1038/nrm3293.
[23] Xu DJ, Liu LB, Zhao YJ, Yang L, Cheng JY, Hua RM, et al. Melatonin protects mouse testes from palmitic acid-induced lipotoxicity by attenuating oxidative stress and DNA damage in a SIRT1-dependent manner. J Pineal Res 2020;69:. doi: https://doi.org/10.1111/jpi.12690e12690.
[24] Lain S, Hollick JJ, Campbell J, Staples OD, Higgins M, Aoubala M, et al. Discovery, in vivo activity, and mechanism of action of a small-molecule p53 activator. Cancer Cell 2008;13:454–63. doi: https://doi.org/10.1016/j.ccr.2008.03.004.
[25] Tseng SH, Lin SM, Chen JC, Su YH, Huang HY, Chen CK, et al. Resveratrol suppresses the angiogenesis and tumor growth of gliomas in rats. Clin Cancer Res 2004;10:2190–202. doi: https://doi.org/10.1158/1078-0432.ccr-03-0105.
[26] Han B, Li SY, Lv YY, Yang DQ, Li JY, Yang QY, et al. Dietary melatonin attenuates chromium-induced lung injury via activating the Sirt1/Pgc-1α /Nrf2 pathway. Food Funct 2019;10:5555–65. doi: https://doi.org/10.1039/c9fo01152h.
[27] Li SY, Baiyun RQ, Lv ZJ, Li JY, Han DX, Zhao WY, et al. Exploring the kidney hazard of exposure to mercuric chloride in mice: disorder of mitochondrial dynamics induces oxidative stress and results in apoptosis. Chemosphere 2019;234:822–9. doi: https://doi.org/10.1016/j.chemosphere.2019.06.096.
[28] Wang XL, Tan ZQ, Chen SD, Gui L, Li XC, Ke D, et al. Norethindrone causes cellular and hepatic injury in zebrafish by compromising the metabolic processes associated with antioxidant defence: Insights from metabolomics. Chemosphere 2021;275:. doi: https://doi.org/10.1016/j.chemosphere.2021.130049130049.
[29] Zhang ZG, Guo CM, Jiang HJ, Han B, Wang XQ, Li SY, et al. Inflammation response after cessation of chronic arsenic exposure and post-treatment of natural astaxanthin in liver: potential role of cytokine mediated cell-cell interactions. Food Funct 2020;11:9252–62. doi: https://doi.org/10.1039/d0fo01223h.
[30] Yang DQ, Han B, Baiyun RQ, Lv ZJ, Wang XQ, Li SY, et al. Sulforaphane attenuates hexavalent chromium-induced cardiotoxicity the activation of the Sesn2/AMPK/Nrf2 signaling pathway. Metallomics 2020;12:2009–20. doi: https://doi.org/10.1039/d0mt00124d.
[31] Yang DQ, Yang QY, Fu N, Li SY, Han B, Liu Y, et al. Hexavalent chromium induced heart dysfunction via Sesn2-mediated impairment of mitochondrial function and energy supply. Chemosphere 2020;264:. doi: https://doi.org/10.1016/j.chemosphere.2020.128547128547.
[32] Narayan N, Lee IH, Borenstein R, Sun JH, Wong R, Tong G, et al. The NAD-dependent deacetylase SIRT2 is required for programmed necrosis. Nature 2012;492:199–204. doi: https://doi.org/10.1038/nature11700.
[33] Wang Y, Mu Y, Zhou XR, Ji HX, Gao X, Cai WW, et al. SIRT2-mediated FOXO3a deacetylation drives its nuclear translocation triggering FasL-induced cell apoptosis during renal ischemia reperfusion. Apoptosis 2017;22:519–30. doi: https://doi.org/10.1007/s10495-016-1341-3.
[34] Li SY, Jiang HJ, Han B, Kong T, Lv YY, Yang QY, et al. Dietary luteolin protects against renal anemia in mice. J Funct Foods 2020:. doi: https://doi.org/10.1016/j.jff.2019.103740103740.
[35] Guida N, Laudati G, Anzilotti S, Sirabella R, Cuomo O, Brancaccio P, et al. Methylmercury upregulates RE-1 silencing transcription factor (REST) in SH-SY5Y cells and mouse cerebellum. Neurotoxicology 2016;52:89–97. doi: https://doi.org/10.1016/j.neuro.2015.11.007.
[36] Sarikhani M, Mishra S, Desingu PA, Kotyada C, Wolfgeher D, Gupta MP, et al. SIRT2 regulates oxidative stress-induced cell death through deacetylation of c-Jun NH-terminal kinase. Cell Death Differ 2018;25:1638–56. doi: https://doi.org/10.1038/s41418-018-0069-8.
[37] Xie Z, Zhao Z, Yang X, Pei LG, Luo HW, Ni QB, et al. Prenatal nicotine exposure intergenerationally programs imperfect articular cartilage via histone deacetylation through maternal lineage. Toxicol Appl Pharmacol 2018;352:107–18. doi: https://doi.org/10.1016/j.taap.2018.03.018.
[38] Zhang Q, Lenardo MJ, Baltimore D. 30 Years of NF-κB: A blossoming of relevance to human pathobiology. Cell 2017;168:37–57. doi: https://doi.org/10.1016/j.cell.2016.12.012.
[39] Nopparat C, Sinjanakhom P, Govitrapong P. Melatonin reverses HO-induced senescence in SH-SY5Y cells by enhancing autophagy via sirtuin 1 deacetylation of the RelA/p65 subunit of NF-κB. J Pineal Res 2017 63.. doi: https://doi.org/10.1111/jpi.12407.
[40] Yeung F, Hoberg JE, Ramsey CS, Keller MD, Jones DR, Frye RA, et al. Modulation of NF-kappaB-dependent transcription and cell survival by the SIRT1 deacetylase. EMBO J 2004;23:2369–80. doi: https://doi.org/10.1038/sj.emboj.7600244.
[41] Al-Haj L, Khabar KSA. The intracellular pyrimidine 5'-nucleotidase NT5C3A is a negative epigenetic factor in interferon and cytokine signaling. Sci Signal 2018:11. doi: https://doi.org/10.1126/scisignal.aal2434.
[42] Gan HQ, Shen T, Chupp DP, Taylor JR, Sanchez HN, Li X, et al. B cell Sirt1 deacetylates histone and non-histone proteins for epigenetic modulation of AID expression and the antibody response. Sci Adv 2020;6:eaay2793. doi: https://doi.org/10.1126/sciadv.aay2793.
[43] Deng ZT, Jin JW, Wang ZH, Wang Y, Gao Q, Zhao JN. The metal nanoparticle-induced inflammatory response is regulated by SIRT1 through NF-κB deacetylation in aseptic loosening. Int J Nanomedicine 2017;12:3617–36. doi: https://doi.org/10.2147/IJN.S124661.
[44] Lu JJ, Jiang HJ, Liu BY, Baiyun RQ, Li SY, Lv YY, et al. Grape seed procyanidin extract protects against Pb-induced lung toxicity by activating the AMPK/Nrf2/p62 signaling axis. Food Chem Toxicol 2018;116:59–69. doi: https://doi.org/10.1016/j.fct.2018.03.034.
[45] Duan WX, He MD, Mao L, Qian FH, Li YM, Pi HF, et al. NiO nanoparticles induce apoptosis through repressing SIRT1 in human bronchial epithelial cells. Toxicol Appl Pharmacol 2015;286:80–91. doi: https://doi.org/10.1016/j.taap.2015.03.024.
[46] Zhao XY, Liu YM, Zhu GL, Liang YY, Liu B, Wu YF, et al. SIRT1 downregulation mediated Manganese-induced neuronal apoptosis through activation of FOXO3a-Bim/PUMA axis. Sci Total Environ 2019;646:1047–55. doi: https://doi.org/10.1016/j.scitotenv.2018.07.363.

[47] Kubben N, Zhang WQ, Wang LX, Voss TC, Yang JP, Qu J, et al. Repression of the antioxidant NRF2 pathway in premature aging. Cell 2016;165:1361–74. doi: https://doi.org/10.1016/j.cell.2016.05.017.
[48] Li SQ, Zhao GJ, Chen LW, Ding YW, Lian J, Hong GL, et al. Resveratrol protects mice from paraquat-induced lung injury: The important role of SIRT1 and NRF2 antioxidant pathways. Mol Med Rep 2016;13:1833–8. doi: https://doi.org/10.3892/mmr.2015.4710.
[49] Huang KP, Huang J, Xie X, Wang SG, Chen C, Shen XY, et al. Sirt1 resists advanced glycation end products-induced expressions of fibronectin and TGF-β1 by activating the Nrf2/ARE pathway in glomerular mesangial cells. Free Radic Biol Med 2013;65:528–40. doi: https://doi.org/10.1016/j.freeradbiomed.2013.07.029.
[50] Ding YW, Zhao GJ, Li XL, Hong GL, Li MF, Qiu QM, et al. SIRT1 exerts protective effects against paraquat-induced injury in mouse type II alveolar epithelial cells by deacetylating NRF2 *in vitro*. Int J Mol Med 2016;37:1049–58. doi: https://doi.org/10.3892/ijmm.2016.2503.
[51] Matsuzaki T, Alvarez-Garcia O, Mokuda S, Nagira K, Olmer M, Gamini R, et al. FoxO transcription factors modulate autophagy and proteoglycan 4 in cartilage homeostasis and osteoarthritis. Sci Transl Med 2018 10.. doi: https://doi.org/10.1126/scitranslmed.aan0746.
[52] El-Ghaiesh SH, Bahr HI, Ibrahiem AT, Ghorab D, Alomar SY, Farag NE, et al. Metformin Protects from rotenone-induced nigrostriatal neuronal death in adult mice by activating AMPK-FOXO3 signaling and mitigation of angiogenesis. Front Mol Neurosci 2020;13:84. doi: https://doi.org/10.3389/fnmol.2020.00084.
[53] Li Z, Bridges B, Olson J, Weinman SA. The interaction between acetylation and serine-574 phosphorylation regulates the apoptotic function of FOXO3. Oncogene 2017;36:1887–98.
[54] Guo YB, Ye Q, Deng P, Cao YN, He DH, Zhou ZH, et al. Spermine synthase and MYC cooperate to maintain colorectal cancer cell survival by repressing Bim expression. Nat Commun 2020;11:3243. doi: https://doi.org/10.1038/s41467-020-17067-x.
[55] Brunet A, Sweeney LB, Sturgill JF, Chua KF, Greer PL, Lin YX, et al. Stress-dependent regulation of FOXO transcription factors by the SIRT1 deacetylase. Science 2004;303:2011–5. doi: https://doi.org/10.1126/science.1094637.
[56] Sang YQ, Li WZ, Zhang GY. The protective effect of resveratrol against cytotoxicity induced by mycotoxin, zearalenone. Food Funct 2016;7:3703–15. doi: https://doi.org/10.1039/c6fo00191b.